

AN. INVESTIGATION OF THE MOHO TOPOGRAPHY BENEATH THE  
MARMARA REGION FROM THE AZIMUTHAL ANOMALIES

AZİMUTAL ANOMALİLERE GÖRE MARMARA BÖLGESİNDE MOHO  
SÜREKSİZLİĞİNİN GÖRECELİ TOPOĞRAFYASI

M.F., ÖZER\*, T. TAYMAZ\*\* and Ö. KENAR\*

\* Department of Geophysical Engineering, Kocaeli University, 41300-Kocaeli

\*\* Department of Geophysical Engineering, İstanbul Technical University, 80626  
Maslak-İstanbul

**Key works:** Marmara Sea, Seismological studies, Azimuthal anomalies.

**Abstract**

Accurate determinations of particle motions is a powerful tool in the investigation of seismic wave propagation. In these studies, the medium is assumed to be homogeneous and isotropic. While the medium is getting more heterogeneous and anisotropic, some deviations are observed in polarization properties, angle of incidence and azimuth of the seismic waves.

Therefore, information about the medium such as heterogeneity and anisotropy could be obtained from particle motion diagrams. We have tried to determine the azimuthal anomalies of the region from the P-wave particle motions using three component short-period seismograms recorded from numerous earthquakes occurred in the vicinity of the Sea of Marmara.

Azimuthal anomalies are generally considered to be related to lateral heterogeneities with the mediums. We have interpreted them in the sense of three dimensional dipping discontinuity (Moho) under the epicentre. Relative topography of the Moho discontinuity beneath the Marmara Region has been obtained using this new assumption.

## Introduction

The Sea of Marmara is a marine basin in northwest Turkey that connects the Aegean Sea with the Black Sea. It is 275 km long and 80 km wide with a broad shallow shelf to the south and a series of deep (up to 1250 m) subbasins to the North (Smith et al. 1995). The Sea of Marmara is located at the western end of the North Anatolian fault. Across most of the Turkey the North Anatolian fault is a relatively simple, narrow, right-slip fault zone; however, it splits into several fault strands in the vicinity of Sea of Marmara so that the deformation becomes distributed over an ~120 km broad zone (Şengör et al., 1985; Barka and Kadinsky-Cade, 1988; Suzanne et al., 1990). The distributed deformation continues to the west across the North Aegean (Taymaz et al. 1991). Numerous damaging earthquakes have affected the Sea of Marmara region in historical time (Ambraseys and Finkel, 1991; Ambraseys, 1988). Both strike-slip and pure normal faulting earthquakes have occurred in the region (Taymaz et al. 1991).

In the seismological studies, a simple structure model consists of homogeneous, isotropic and horizontal layers overlying the half space is taken, and plane waves are used in order to help computing. In such a simple model, P-waves propagate in a vertical plane between the source and station, and their particle motion is linear along the ray path. Therefore, vertical-radial (Z-R) and NS-EW diagrams of the P-wave particle motions give the apparent incidence and azimuth angles, respectively. Clearly, this known particle motion will change when the medium is heterogeneous and anisotropic. This property provides the particle motions to be used in for determining the heterogeneity and anisotropy of a region. For example, if there dipping layers, refracted and reflected waves deviate from the source-station vertical plane, i.e. deviations take place in the apparent incidence and azimuth angles of the waves. Deviation in the azimuthal angle is called as *the azimuthal anomaly*, which can be used to determine the topography of discontinuities along which the waves propagate. In this study, topography of the Moho beneath the Marmara region has been investigated from observations of the azimuthal anomalies in Pn-waves. Azimuthal anomalies can be determined from both the polarization analysis and particle motion diagrams. Basa et al. (1994), have given a good example for polarization analysis in which azimuth of the incident wave is estimated. We have determined the azimuthal anomalies directly from the particle motion diagrams.

### Determination of the Azimuthal Anomalies From the Particle Motion Diagrams

Since the P-wave particle motion is along the ray path, if the azimuth computed from the coordinates of the station and source is true, maximum and minimum wave amplitudes have to be on the radial (R) and tangential (T) components, respectively.

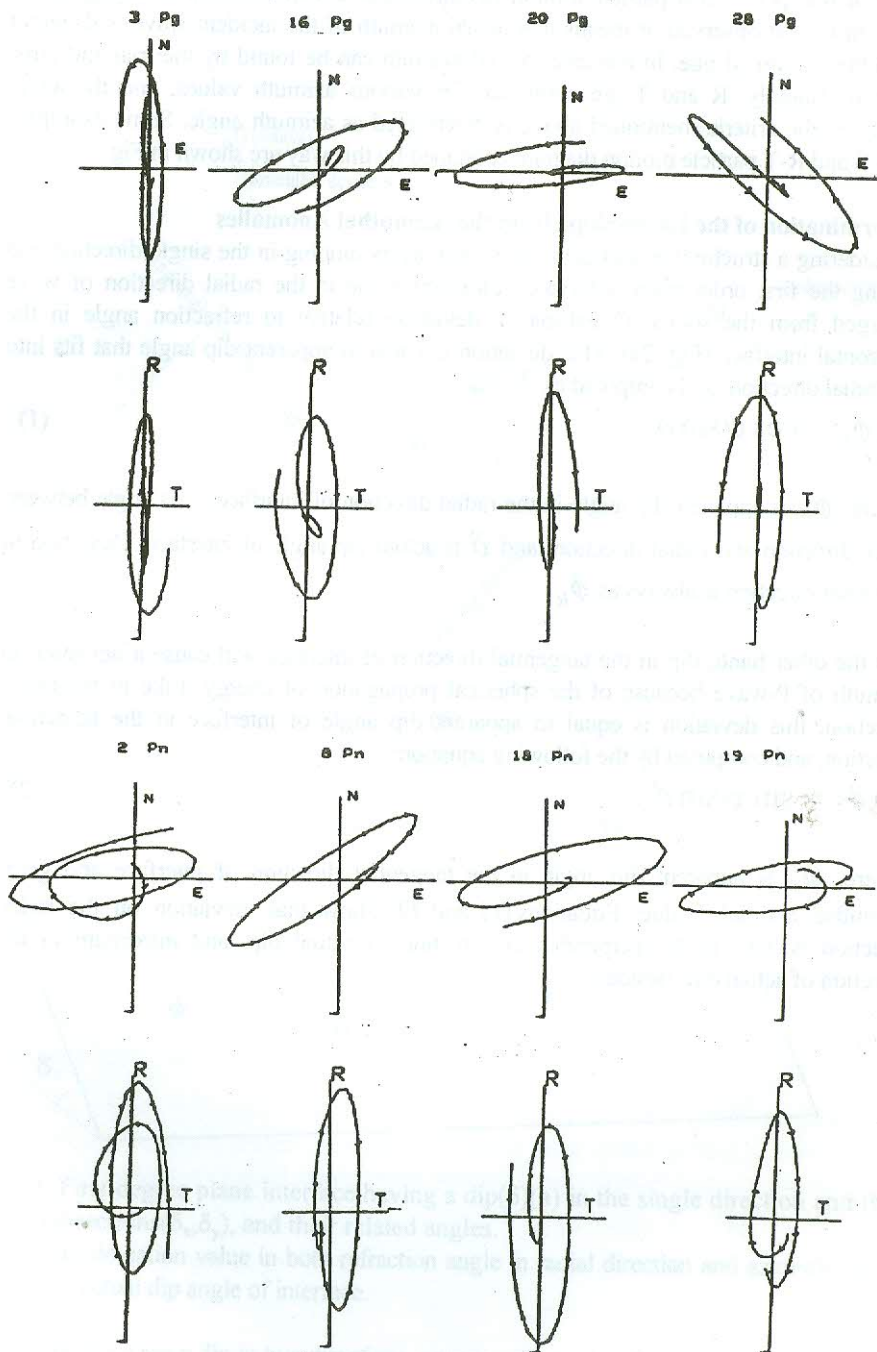


Fig. 1. The particle motion diagrams for earthquakes studied. Earthquake numbers in Table 1 and their first arrivals are at top of diagrams. N-E diagrams are unrotated, and their rotated diagrams are plotted at the bottom.

Thus, it is expected that particle motion fits into radial direction on the R-T diagram. If this can not be observed, it means that actual azimuth of the incident wave is different from the computed one. In this case, actual azimuth can be found by the trial and error method. Namely, R and T are computed for various azimuth values, and the angle satisfying the criteria mentioned above is determined as azimuth angle. Some examples of N-S and R-T particle motion diagrams obtained by this way are shown in Fig. 1.

#### Determination of the Layer Slope from the Azimuthal Anomalies

Considering a structural model consists of two layers dipping in the single direction and having the first order plane interface, refraction angle in the radial direction of wave emerged from the source O exhibits a deviation relative to refraction angle in the horizontal interface (Fig. 2a). This deviation is equal to apparent dip angle that fits into the radial direction, and computed as

$$\sin \phi_R = \cos \psi \sin \delta \quad (1)$$

Where,  $\phi_R$  is apparent dip angle in the radial direction of interface,  $\psi$  is angle between strike direction and radial direction, and  $\delta$  is actual dip angle of interface. Deviation in the radial direction is always as  $\phi_R$ .

On the other hand, dip in the tangential direction of interface will cause a deviation in azimuth of P-wave because of the spherical propagation of energy. Like in the radial direction, this deviation is equal to apparent dip angle of interface in the tangential direction, and computed by the following equation;

$$\sin \phi_T = \sin \psi \sin \delta \quad (2)$$

Where,  $\phi_T$  is apparent dip angle in the tangential direction of interface and gives azimuthal anomaly value. Equations (1) and (2) show that deviation on the radial direction is zero in the perpendicular direction to actual dip, and maximum in the direction of actual dip. Besides,

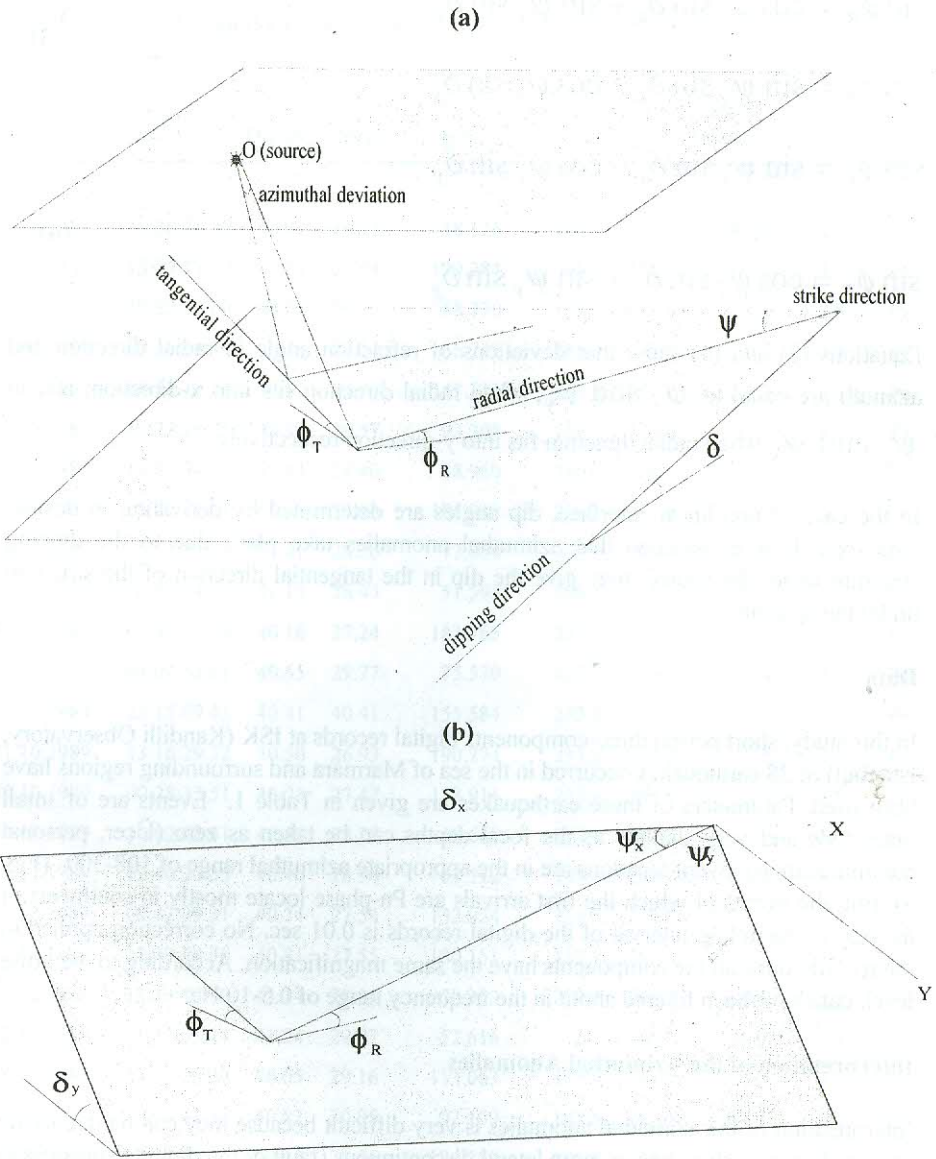


**Fig. 2.** First degree plane interface having a dip( $\delta$ )(a) in the single direction and (b) in two directions( $\delta_x, \delta_y$ ), and their related angles. maximum deviation value in both refraction angle in radial direction and azimuth angle will be as actual dip angle of interface.

When interface has a dip in two directions, apparent dip angles (Fig. 2b) are computed by the following equations;

$$\sin \phi_R = \cos \psi_x \sin \delta_x + \sin \psi_x \sin \delta_y \quad (3)$$

$$\sin \phi_R = \sin \psi_y \sin \delta_x + \cos \psi_y \sin \delta_y$$

$$\sin \phi_T = \sin \psi_x \sin \delta_x + \cos \psi_x \sin \delta_y \quad (4)$$

$$\sin \phi_T = \cos \psi_y \sin \delta_x + \sin \psi_y \sin \delta_y$$

Equations (3) and (4) show that deviations of refraction angle in radial direction and azimuth are equal to  $\psi_x$  and  $\psi_y$ , when radial direction fits into x-direction, and to  $\psi_y$  and  $\psi_x$  when radial direction fits into y-direction respectively.

In the case of non-linear interface, dip angles are determined by derivating in desired directions. If it is assumed that azimuthal anomalies take place due to the dipping structure under the source, they give the dip in the tangential direction of the structure under the epicentre.

#### Data

In this study, short period three-components digital records at ISK (Kandilli Observatory, İstanbul) of 28 earthquakes occurred in the sea of Marmara and surrounding regions have been used. Parameters of these earthquakes are given in Table 1. Events are of small magnitude and very shallow as the focal depths can be taken as zero (Üçer, personal communication). Event locations are in the appropriate azimuthal range of 108-300 (Fig. 3). But, the events of which the first arrivals are Pn-phase locate mostly in southwest of the region. Sampling interval of the digital records is 0.01 sec. No correction applied to the records since all the components have the same magnification. According to the noise level, data have been filtered about in the frequency range of 0.5-10 Hz.

#### Interpretation of the Azimuthal Anomalies

Interpretation of the azimuthal anomalies is very difficult because they can be due to the various factors such as one or more lateral discontinuous (fault or the dipping subsurface) between source and receiver, local heterogeneity along the ray path and anisotropic medium. For that

**Table 1.** Earthquake parameters and azimuthal anomalies.

No	Date	Origin Time (to)	Lat. (North)	Lon (East)	$\Delta$ (km)	Az.*	Az.**	Az. Anomaly	$M_L$	First Arrival
1	29.08.1989	16:28:36.29	40.91	29.13	18.126	161.0	120.0	-41.0?	2.5	Pg
2	03.09.1989	13:27:17.20	41.04	27.64	119.284	269.1	258.0	-11.1	3.2	Pn
3	07.09.1989	19:22:52.60	40.27	29.17	88.770	173.9	178.0	4.1	2.8	Pg
4	07.09.1989	20:36:54.46	40.48	29.24	66.742	166.7	176.5	9.8	3.3	Pg
5	10.09.1989	08:32:19.34	40.47	27.50	147.222	243.8	253.0	9.2	3.5	Pn
6	10.09.1989	10:22:25.95	40.32	29.57	93.308	152.3	176.0	23.7	2.9	Pg
7	23.09.1989	18:30:34.87	40.44	28.40	88.960	218.9	224.9	5.1	3.0	Pg
8	30.09.1989	00:47:17.41	40.13	27.24	185.633	236.6	234.0	-2.6	3.7	Pn
9	02.10.1989	15:24:13.46	41.41	28.26	77.089	300.0	265.0	-35.0?	2.8	Pg
10	03.10.1989	10:06:54.37	41.13	28.45	51.596	278.2	265.5	-12.7	2.9	Pg
11	11.10.1989	07:40:55.94	40.16	27.24	183.763	237.4	252.0	14.6	3.1	Pn
12	13.10.1989	04:01:53.61	40.65	29.77	75.570	127.7	141.1	13.4	3.4	Pg
13	15.10.1989	23:15:09.43	40.41	40.41	155.584	242.6	256.0	13.4	2.9	Pn
14	21.10.1989	13:16:29.32	40.50	26.93	190.274	251.5	264.0	12.5	3.7	Pn
15	27.10.1989	00:28:35.51	40.73	27.47	138.914	255.0	252.0	-3.0	2.8	Pn
16	04.11.1989	10:02:12.51	40.88	28.28	68.668	252.8	247.0	-5.8	3.0	Pg
17	06.11.1989	12:40:30.35	40.46	28.96	67.712	187.1	192.1	5.0	3.3	Pg
18	01.12.1989	08:42:39.31	40.74	27.54	132.924	254.5	256.0	1.5	3.4	Pn
19	02.12.1989	21:39:48.36	40.81	27.55	130.151	257.9	257.9	0.0	3.4	Pn
20	04.12.1989	12:19:46.70	41.14	28.44	50.360	279.2	266.0	-13.2	2.7	Pg
21	22.12.1989	11:32:05.74	41.24	29.07	52.616	2.7	346.7	16.0?	2.9	Pg
22	28.12.1989	23:13:29.00	40.05	29.16	113.003	175.6	184.0	8.4	3.5	Pn
23	05.10.1990	10:16:44.46	40.82	30.05	92.109	107.8	142.0	34.2?	3.0	Pg
24	06.10.1990	00:02:25.01	39.45	28.56	184.209	193.5	188.0	-5.5	3.0	Pn
25	06.10.1990	05:52:25.50	40.79	27.85	106.260	253.7	245.0	-8.7	3.2	Pg
26	08.05.1990	05:50:14.15	40.65	30.18	105.094	115.7	114.0	-1.7	3.2	Pg
27	24.10.1990	11:16:43.06	39.82	30.29	173.191	142.6	170.0	27.4?	4.1	Pn
28	04.11.1990	23:39:19.81	40.62	29.95	89.879	123.1	130.0	6.9	3.3	Pg

\* Azimuth from epicentre and station coordinates.

\*\* Azimuth from particle motion diagrams.

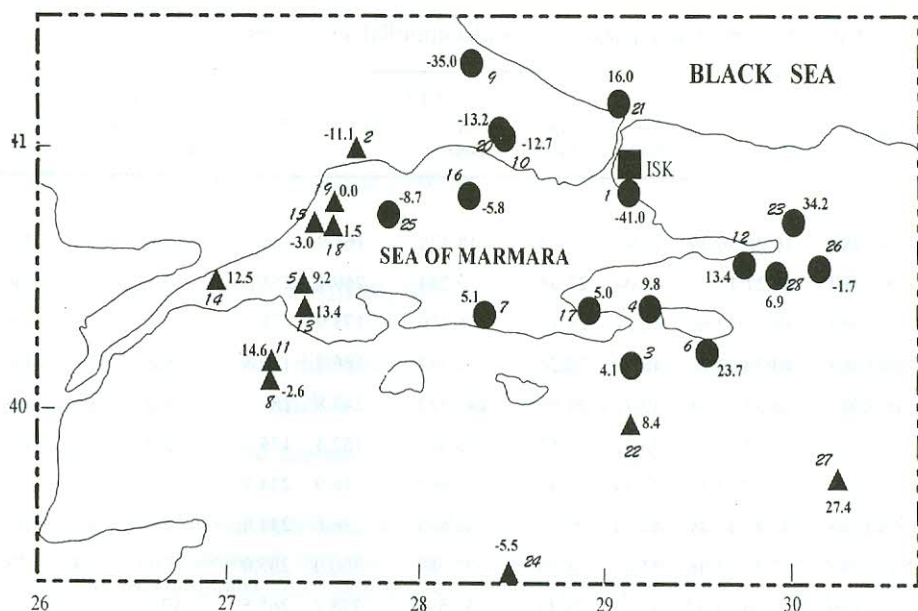


**Fig. 3.** Epicentre locations of the earthquakes,  $\Delta$  for Pn first arrivals and  $\bullet$  for Pg first arrivals. Numbers show the azimuthal anomalies.

reason, the most important point is to make decision which factor is a reason of these anomalies. Origin of the azimuthal anomalies can not be anisotropy or local heterogeneity since the study area is too large. In this case, to look over previous geophysical investigations for the region will be useful.

Canitez (1969) and Osmařahin & Alptekin (1990) have obtained 35 km average crustal thickness for Aegean region using the surface wave data. This results is concern with southern of the Marmara Region. Kenar (1978), have computed about 30 km and 25 km crustal thickness beneath Istanbul for NS and EW directions, respectively using the spectral ratio technique. It means that depth of the Moho differs 5 km from north to south in Bosphorus. Özer and Kenar (1992) has studied crustal structure beneath Istanbul using converted phases in crustal layers and observed significant distortions in the wave form of P-waves on the tangential component, and explained these by the dipping Moho. Finally, Gürbüz et al. (1991) have studied crustal structure in the Marmara Region using P-wave travel time data. They have given variation of the Moho depth in detail for this region. All of these studies show that depth of the Moho discontinuity has significant variations and is increasing southward. Consequently, it will be reasonable to say that the azimuthal anomalies are caused by the dipping Moho. For that reason, azimuthal anomalies have been explained by dipping subsurface under each epicentre in this study.

We have determined azimuthal anomalies for both Pg and Pn first arrivals. Since Pn wave propagates along the Moho discontinuity, their anomalies are belong this interface. There are twelve events of which first arrivals are Pn. Locations of these events except three

numbered as 22, 24 and 27 in Table 1 are in eastern of Dardanelles (Fig. 3). Although distribution of this group is sufficient for this part of region, numbers and distribution of Pn anomalies are insufficient for rest of region. For this region, we have also determined the azimuthal anomalies for Pg first arrivals. These are in a good agreement with the Pn anomalies (Fig. 4). As shown in Fig. 4, all the anomalies except events 1 and 9 are in a certain angular range. For this reason, we can assume that crustal interfaces are parallel to Moho discontinuity. According to this assumption, we have interpreted Pg anomalies as Pn anomalies, and used both of them to compute relative depths of the Moho for the whole region. Since the azimuthal anomalies give apparent dip angles of the Moho in tangential directions under each epicenter, they can be easily transform to the depth differences. For this purpose, we take a crustal model that consists of a horizontal layer overlying half space (Table 2). Taking the thickness of crust (Fig. 5) as the reference level, depth differences ( $h$ ) corresponding to the azimuthal anomalies are computed from

$$\Delta h = \tan(i_c - \phi_T) \cdot \tan \phi_T \quad (5)$$

and added to the reference level.

**Table 2.** The earth model using in computation for relative depths.

	P-wave velocity (km/sec)	Depth (km)
Crust	6.2	27
Upper Mantle	8.1	—

The relative topography map of the Moho has been obtained by contouring the relative depths and shown in Fig. 6. Fig. 7a and b show 3D plots of the Moho beneath Marmara Region. It is shown that there are two ridge axes lying from Bosphorus towards Dardanelles and İznik Lake. Besides, there is a local rise in the mantle beneath İzmit Gulf, and depth of the Moho increases just in south of İzmit Gulf. There is also a small uplift in east of Bursa and a considerable trough just under the Uludağ Mountain. Arising in the mantle at southwest of İzmit Gulf is due to the lack of data for this location. Similar effect of data deficiency seems in north of Trakya and Kocaeli Peninsula. These are consistent with results of the previous investigations mentioned above. Notice that consistency between the Moho and surface topographies satisfies the izostatic equilibrium.

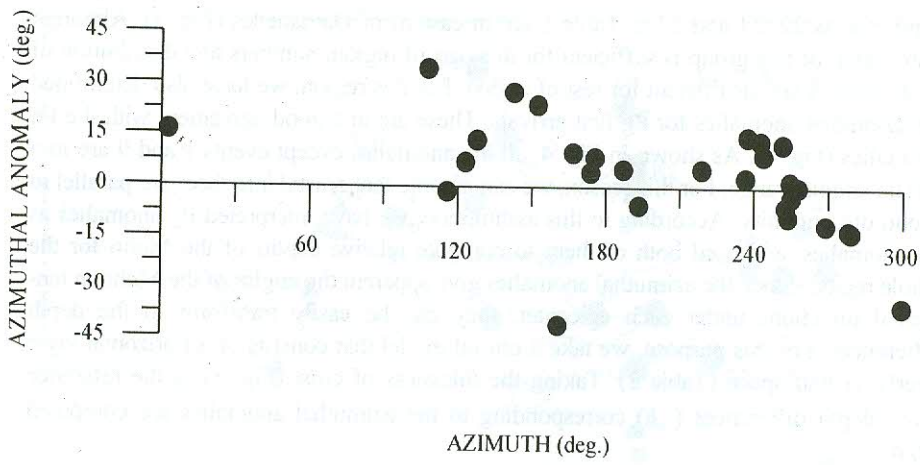


Fig. 4. Distribution of the azimuthal anomalies of earthquakes studied versus azimuth.

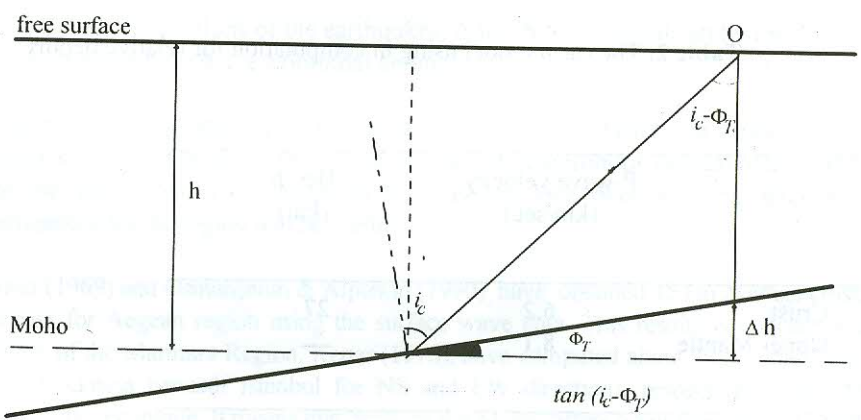


Fig. 5. Depth difference for the dipping Moho.

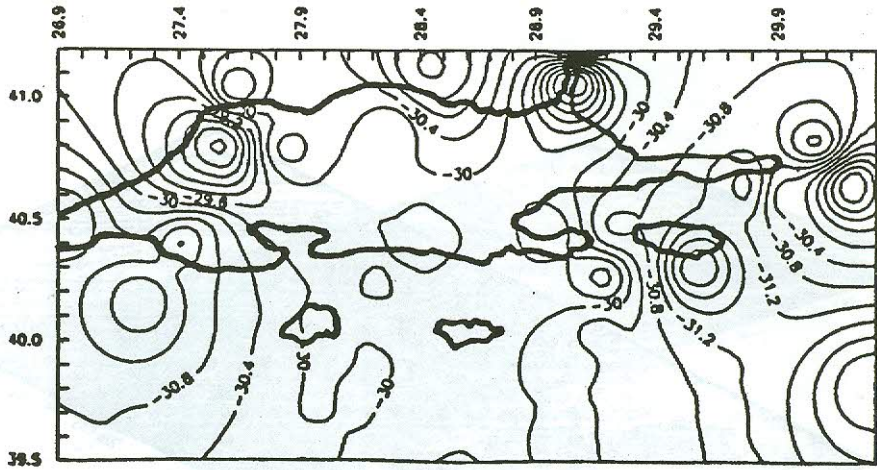


Fig. 6. Map of the Moho topography beneath the Marmara Region.

In spite of deficiency of data, consistencies of these results are amazing. Since some details may seem like over speculation, we fitted first and third degrees surfaces to the relative depths in the least square sense. The estimated Moho discontinuity becomes deeper southwards, and its depth increases in both south-eastern and south-western parts more than that of central Marmara region.

### Conclusions

We have studied 28 earthquakes within the Marmara region to determine the topography of the Moho discontinuity beneath the Marmara region using the azimuthal anomalies computed from the particle motion diagrams. The use of digital data improves accuracy of the anomalies. The results we have obtained are reasonable and consistent with the previous studies in spite of inadequacy of the available data. This brings up the efficiency of the method. It will be better to get more precise results using the sufficient number of data in a good azimuthal coverage. Our results show that the Moho discontinuity in the region gets deeper from north to south and its deepest parts are in southwest and southeast edges.

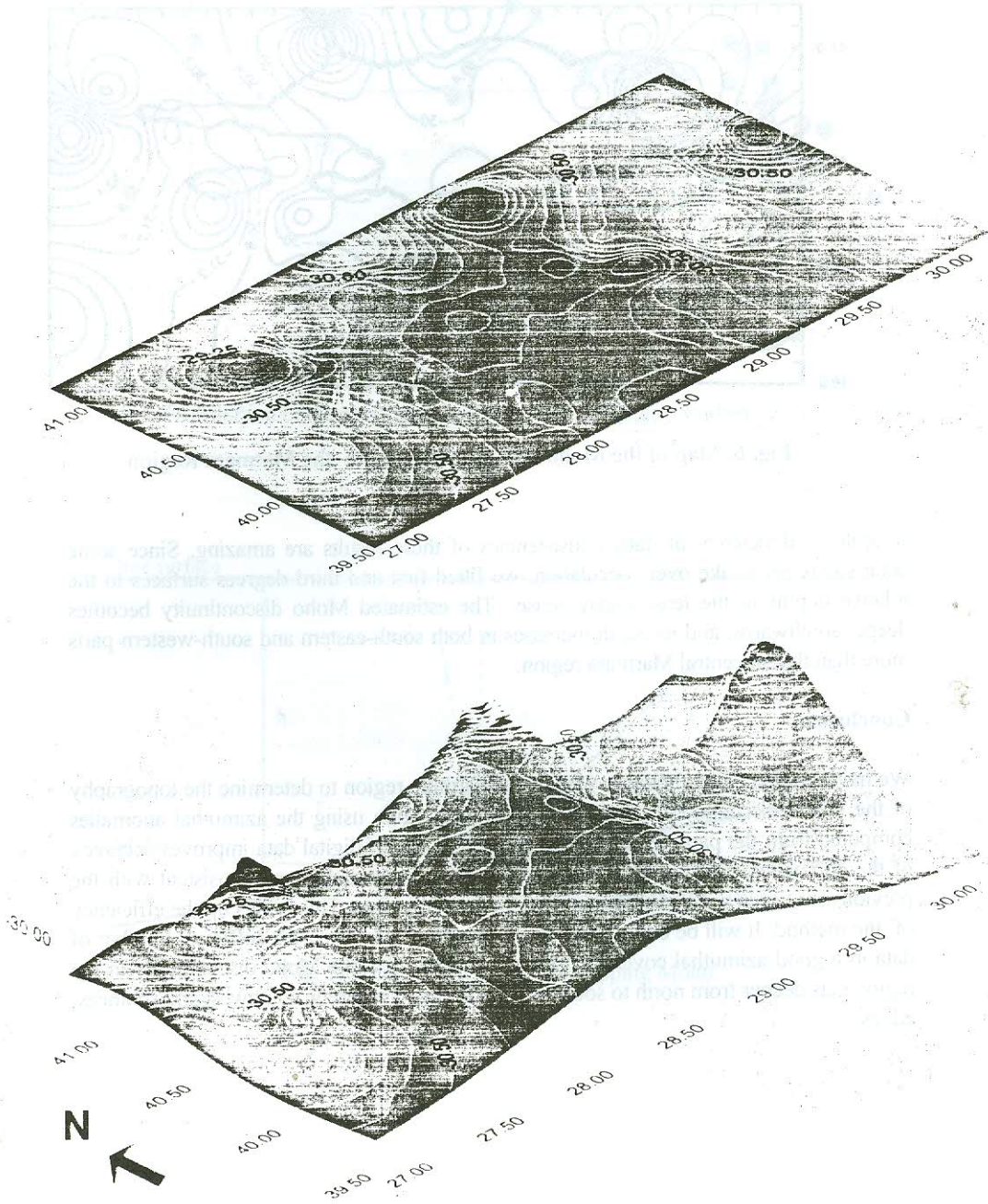


Fig. 7a. 3D plot of relative depths of the Moho in the Marmara Region from South.

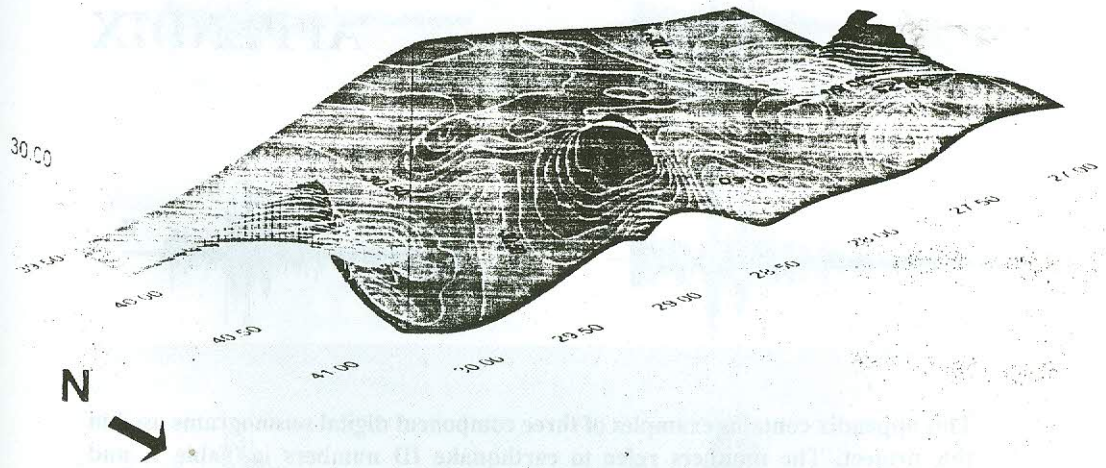
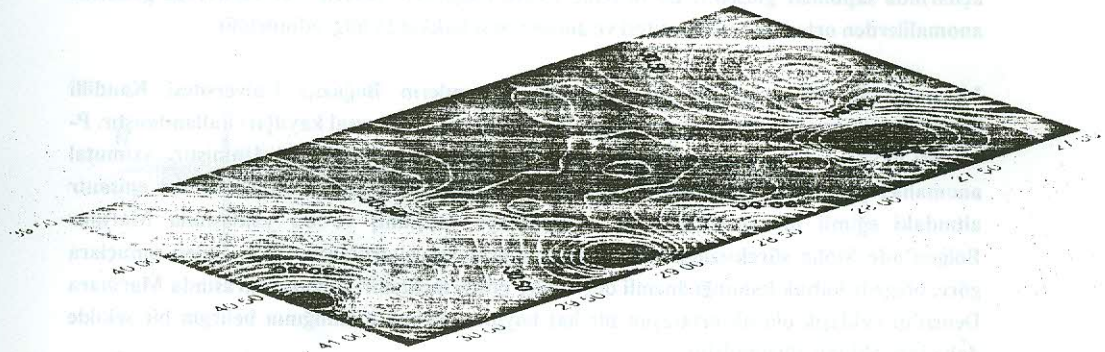


Fig. 7b. 3D plot of relative depths of the Moho in the Marmara Region from North.

## Özet

Sismik dalga yayınımmının incelenmesinde tanecik hareketlerinin belirlenmesi etkin bir yoldur. Bu tür çalışmalarda ortam homojen ve izotrop varsayılmaktadır. Ortamın heterojenliği ve anizotropisi arttıkça, sismik dalgaların hem polarizasyonunda, hem de geliş ve azimut açılarında sapmalar gözlenir. Bu nedenle sismik dalgaların tanecik hareketlerinde gözlenen anomalilerden ortamın heterojenitesi ve anizotropisi hakkında bilgi edinilebilir.

Marmara Denizi civarında oluşmuş bazı depremlerin Boğaziçi Üniversitesi Kandilli Rasathanesi sismoloji istasyonuna ait üç bileşen kısa-periyod sayısal kayıtları kullanılmıştır. P-dalgası ilkvarışlarının tanecik hareketlerinden azimutal anomaliler belirlenmiştir. Azimutal anomaliler yanal doğrultudaki heterojenlikle ilişkilidir. Hesaplanan bu anomaliler episantr altındaki eğimli bir süreksizlik ile açıklanmaya çalışılmış ve bu yaklaşımla Marmara Bölgesi'nde Moho süreksizliğinin göreceli topografyası çıkarılmıştır. Elde edilen sonuçlara göre, bölgede kabuk kalınlığı önemli değişimler göstermektedir. Boğazlar arasında Marmara Denizi'ni yaklaşık olarak ortlayan bir hat boyunca kabuk kalınlığının belirgin bir şekilde daha ince olduğu görülmüştür.

## Acknowledgements

We would like thank to Balamir Üçer and his colleagues in Kandilli Observatory, Bosphorus University, for making their data archive available. This paper is a part of the National Marine Geology and Geophysics Project (Coordinator Naci Görür) supported by Scientific and Technical Research Council of Turkey (TÜBİTAK) through grant number YDABÇAG-235/G.

## APPENDIX

This appendix contains examples of three component digital seismograms used in this project. The numbers refer to earthquake ID numbers in Table I, and Z, N and E represent vertical, north-south and east-west components respectively. Time scale is also shown below the seismograms.

3

87

20

5

Z



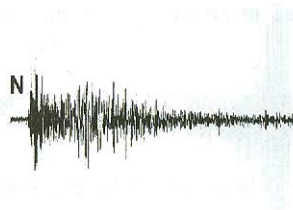
Z



N



N



E



E



16

28

Z



Z



N



N



E



E

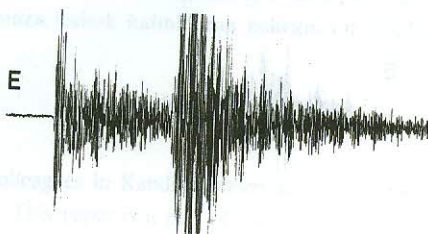


1 min.

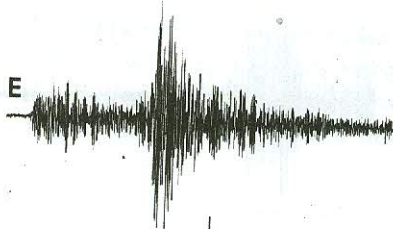
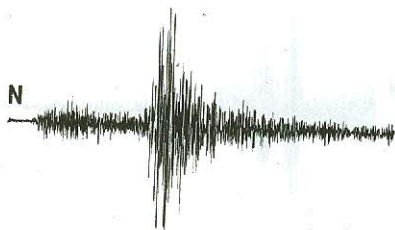
2



18



19



8



1 min.

## References

- Ambraseys, N.N. (1988). Engineering Seismology: *Earthquake Engineering and Structural Dynamics* 17: 1-105.
- Ambraseys, N.N. and Finkel, C.F. (1991). Long-term seismicity of Istanbul and of the Marmara Sea region: *Terra Nova* 3, 527-539.
- Barka, A.A. and Kadinsky-Cade, K. (1988). Strike-slip fault geometry in Turkey and its influence on earthquake activity, *Tectonics* 3: 663-684.
- Basa, H.S., Özer, M.F., Osmañahin, İ and Kenar, Ö. (1994). Üç bileşen sismik verilerin polarizasyon analizi, *Jeofizik* 8: 77-89.
- Canitez, N. (1969). Türkiye ve civarındaki depremlere ait fundamental moddan yüzey dalgaları üzerine incelemeler, *Proje: TÜBİTAK MAG-150*.
- Gürbüz, C., Püskülcü, S. and Üçer, S.B. (1991). A study of crustal structure in the Marmara Region using earthquake data, *Bull. Bosphorus Univ. Report* 4: 29-41.
- Kenar, Ö. (1978). Sismik P dalgalarının genlik spektrumlarından yararlanarak İstanbul ve civarında yer kabuğu yapısı, *PhD Thesis, Istanbul Technical University*.
- Osmañahin, İ. and Alptekin, Ö. (1990). Love ve Rayleigh dalgalarının istasyonlar arası ortam tepki fonksiyonlarından Anadolu ve civarında kabuk ve üst-manto yapısının belirlenmesi, *Jeofizik* 4: 123-146.
- Özer, M.F. and Kenar, Ö. (1992). Dönüşmüş fazlarla İstanbul civarında yer kabuğu yapısının modellenmesi, *Jeofizik* 6: 113-124.
- Smith, A.D., Taymaz, T., Oktay, F., Yüce, H., Alpar, B., Başaran, H., Jackson, J., Kara, S. and Şimşek, M. (1995). High-resolution seismic profiling in the Sea of Marmara (northwest Turkey): Late Quaternary sedimentation and sea-level changes, *Geological Society of America Bulletin* 107-8: 923-936.
- Suzanne, P., Lyberis, N., Chorowicz, J., Nurlu, M., Yurur, T. and Kasapoğlu, E. (1990). La geometrie de la faille norde-anatolienne a partir d'images Landsat-MSS, *Bulletin de la Societe Geologique de France* 8: 589-599.
- Şengör, A.M.C., Görür, N. and Şaroğlu, F. (1985). Strike-slip faulting and related basin formation in zones of tectonic escape: Turkey as a case study, in Biddle, K.T., and Christie-Blick, N., eds., *Strike-slip deformation, basin formation and sedimentation, Society of Economic Paleontologists and Mineralogists Special publication* 37: 227-264.
- Taymaz, T., Jackson, J. A. and Mc Kenzie, D.P. (1991). Active tectonics of the north and central Aegean Sea. *Geophysical Journal International* 106: 433-490.

Accepted 29.8.1996